

## Double-injection method for sequentially measuring cerebral blood flow with N-isopropyl-( $^{123}\text{I}$ )p-iodoamphetamine

Kenya MURASE,\* Takeshi INOUE,\*\* Hiroyoshi FUJIOKA,\*\* Yuji YAMAMOTO\*\*\* and Junpei IKEZOE\*\*\*\*

\*Department of Medical Engineering, Division of Allied Health Sciences, Osaka University Medical School

\*\*Department of Radiology, Matsuyama Shimin Hospital

\*\*\*Department of Neurosurgery, Matsuyama Shimin Hospital

\*\*\*\*Department of Radiology, Ehime University School of Medicine

We investigated the accuracy of a double-injection method for sequentially measuring cerebral blood flow (CBF) with N-isopropyl-( $^{123}\text{I}$ )p-iodoamphetamine (IMP) in simulation studies based on patient data and in clinical studies. The unidirectional clearance of IMP from the blood to the brain ( $K_1$ ; nearly equal to CBF) in the first and second sessions was calculated by means of a microsphere model. The  $K_1$  values in the first session ( $K_1^I$ ) were calculated from  $C_b(5)/\text{Int\_}C_a^I$ , where  $C_b(5)$  and  $\text{Int\_}C_a^I$  are values for brain radioactivity 5 min after the first injection and for arterial blood radioactivity obtained by 5-min continuous sampling. The  $K_1$  values in the second session ( $K_1^{II}$ ) were calculated by means of the following four methods. Method 1:  $[C_b(t_z + 5) - C_b(t_z)]/[\text{Int\_}C_a^{II} - C_a(t_z) \times 5]$ , where  $C_b(t_z + 5)$  and  $C_b(t_z)$  are the brain radioactivity levels 5 min after the second injection and at the time the second session was started ( $t_z$ ), respectively.  $\text{Int\_}C_a^{II}$  and  $C_a(t_z)$  are the arterial blood radioactivity levels obtained by 5-min continuous sampling after the second injection and at  $t_z$ , respectively. Method 2:  $[C_b(t_z + 5) - C_b(t_z)]/[\text{Int\_}C_a^I \times R]$ , where  $R$  is the injection dose ratio. Method 3:  $[C_b(t_z + 5) - C_b(t_z) \times \exp(-K_1^I \times 5/\lambda)]/\text{Int\_}C_a^{II}$ , where  $\lambda$  is the population averaged partition coefficient. Method 4: same as Method 3 except that  $K_1^I$  was replaced by  $K_1^{II}$  obtained by means of Method 2. Theoretically, Method 4 appeared to be the best of the four methods. The change in  $K_1$  during the second session obtained by Method 1 or 2 largely depended on  $R$  and  $t_z$ , whereas Method 3 or 4 yielded a more reliable estimate than Method 1 or 2, without largely depending on  $R$  and  $t_z$ . Since Method 2 was somewhat superior to other methods in terms of noninvasiveness and simplicity, it also had the potential for routine clinical use. The reproducibility of two sequential measurements of  $K_1$  was investigated with clinical data obtained without any intervention. The response of CBF to acetazolamide challenge was also assessed by the above four methods. The knowledge gained by this study may assist in selecting a method for sequentially measuring CBF with a double injection of IMP.

**Key words:** double-injection method, N-isopropyl-( $^{123}\text{I}$ )p-iodoamphetamine, cerebral blood flow, SPECT

### INTRODUCTION

N-isopropyl-( $^{123}\text{I}$ )p-iodoamphetamine (IMP) is a widely

applied brain imaging agent that was synthesized and recommended for use as a tracer of cerebral perfusion.<sup>1</sup> More recently, Kuhl et al.<sup>2</sup> have used intravenously injected IMP with arterial blood sampling to demonstrate a local correlation between IMP and microsphere trapping in dog brain samples, and have extended this model to measurements of local cerebral blood flow (CBF) in humans by means of single photon emission computed tomography (SPECT). IMP is highly extracted by the brain and has good linearity between its uptake and CBF.<sup>2</sup>

Received May 9, 2000, revision accepted September 28, 2000.

For reprint contact: Kenya Murase, Dr. Eng., Dr. Med. Sci., Department of Medical Engineering, Division of Allied Health Sciences, Osaka University Medical School, 1-7 Yamadaoka, Suita, Osaka 565-0871, JAPAN.

E-mail: murase@sahs.osaka-u.ac.jp

To understand the pathophysiology of cerebrovascular disease, it is very useful in assessing perfusion reserve.<sup>3,4</sup> The response of the cerebral circulation to pharmacological intervention such as carbon dioxide inhalation or acetazolamide (ACZ) injection has been investigated to assess perfusion reserve. To evaluate these effects on CBF, repeated CBF quantitation with and without pharmacological intervention, is necessary.<sup>5</sup> Various cerebral perfusion agents have been utilized in combination with ACZ.<sup>6-8</sup> It is known that IMP is sensitive to ACZ challenge because of its superior linearity against CBF.<sup>5</sup> Although technetium-99m compounds such as <sup>99m</sup>Tc-HMPAO and <sup>99m</sup>Tc-ECD have also been widely used for assessment of cerebral perfusion in clinical settings, ACZ loading has not been successful because of the nonlinear relationship between regional tracer uptake and CBF.<sup>7,8</sup>

IMP SPECT with arterial blood sampling is superior in reproducibility and has become a standard method for CBF measurement.<sup>2</sup> As pointed out by Hashikawa et al.,<sup>5</sup> two IMP SPECT studies should be performed at an interval of at least several days, and double invasive catheterization is required for assessing perfusion reserve with IMP and pharmacological intervention. To overcome these drawbacks, Hashikawa et al.<sup>5</sup> developed split dose IMP SPECT, which enables CBF quantitation under two conditions in a short time with a single arterial catheterization. They quantified absolute CBF values by a reference sample method based on a microsphere model<sup>2</sup> in the first session, and in the second, by a reference sample method with subtraction of the radioactivity remaining due to the first IMP injection. Moriwaki et al.<sup>9</sup> have recently investigated the hemodynamic aspect of cerebral watershed infarction by assessing perfusion reserve with this method. We recently developed a modified early (ME) method which can shorten the total time required for CBF measurement with IMP and a single-head rotating gamma camera, and applied it to split dose IMP SPECT.<sup>10</sup>

IMP uptaken by the brain is gradually washed out from the brain,<sup>11,12</sup> which precludes simple subtraction of the radioactivity due to the first dose, from the second, but the effect of these inherent characteristics of IMP on the accuracy of the quantitative measurement of CBF with a double injection of IMP has not been analyzed in detail. The purpose of the present study was therefore to investigate the accuracy of a double-injection method for sequentially measuring CBF with IMP by simulation studies based on patient data and with experimental data obtained in clinical settings.

In this study, we consider four methods based on a microsphere model for sequentially measuring CBF with a double injection of IMP, and focus upon the effects of the injection dose ratio and the start time of the second session on their accuracy.

## MATERIALS AND METHODS

### Kinetic model

The rate of change of IMP levels in the brain tissue [ $M(t)$ ] is given by the following differential equation:

$$\frac{dM(t)}{dt} = K_1 C_a(t) - k_2 M(t), \quad (1)$$

where  $C_a(t)$  is the amount of IMP radioactivity in the arterial blood at time  $t$ ,  $K_1$  is the unidirectional clearance of IMP from the blood to the brain tissue, and  $k_2$  is the rate constant for back diffusion of IMP from the brain tissue to the blood.  $M(t)$  and  $C_a(t)$  in Eq. (1) are corrected for decay.  $K_1$  is given by the product of the CBF and the extraction fraction of the tracer by the brain tissue. Since the extraction fraction of IMP by the brain tissue is high,<sup>13</sup>  $K_1$  appears to be nearly equal to CBF. The IMP content per unit volume of brain measured by SPECT [ $A(t)$ ] is given by

$$A(t) = M(t) + V_0 C_a(t), \quad (2)$$

where  $V_0$  is the brain vascular volume. In the present study,  $V_0$  was assumed to be negligible. It should be noted that soon after the intravenous injection of IMP, the  $k_2$  value in Eq. (1) can be assumed to be zero, that is, a microsphere model is considered to hold true during this period.

From Eq. (1), the brain tissue radioactivity at time  $t$  [ $A^I(t)$ ] in the first session ( $0 \leq t \leq t_z$ ) is given by

$$A^I(t) = K_1^I \cdot \int_0^t e^{-k_2^I(t-u)} C_a^I(u) du, \quad (3)$$

and the brain tissue radioactivity at time  $t$  [ $A^{II}(t)$ ] in the second session ( $t > t_z$ ) is given by

$$A^{II}(t) = K_1^I \cdot \int_0^{t_z} e^{-k_2^I(t_z-u)} C_a^I(u) du \cdot e^{-k_2^{II}(t-t_z)} + K_1^{II} \cdot \int_{t_z}^t e^{-k_2^{II}(t-u)} C_a^{II}(u) du, \quad (4)$$

where  $t_z$  denotes the end time of the first session or the start time of the second session. In this study, we assumed that each injection of IMP and each session started simultaneously. The superscripts I and II in the above equations denote the first and second sessions, respectively. When formulating the brain tissue radioactivity of IMP in the second session [Eq. (4)], we assumed that the rate constants instantaneously change from the first to the second session.

In the present study, the level of radioactivity in arterial blood [ $C_a(t)$ ] was simulated as

$$C_a(t) = C_a^I(t) + C_a^{II}(t), \quad (5)$$

where  $C_a^I(t)$  and  $C_a^{II}(t)$  are the first and second radioactivity levels in arterial blood, respectively.  $C_a^{II}(t)$  was defined as

$$C_a^{II}(t) = \begin{cases} 0 & \text{for } t \leq t_z, \\ R \cdot C_a^I(t - t_z) & \text{for } t > t_z \end{cases} \quad (6)$$

where  $R$  is the injection dose ratio, that is, the ratio of the second to the first injection dose.

#### Modified early (ME) method

Sufficient SPECT data with a short scan duration are difficult to obtain 5 min after IMP injection with a conventional SPECT scanner because of the low level of radioactivity in the brain. A later SPECT scan of long scan duration is required in which the image should be corrected with the ratio of the change of the entire brain radioactivity level. We developed a method for measuring CBF with IMP and a single-head rotating gamma camera.<sup>10</sup> This procedure is called the modified early (ME) method and it is a modification of the protocol developed by Matsuda et al.<sup>14</sup> Figure 1 shows the protocol when the ME method was applied to split dose IMP SPECT. SPECT data were acquired from 7 to 25 min after each injection of IMP (Fig. 1). When acquiring SPECT data, a gamma camera was rotated twice clockwise and counterclockwise to reduce artifacts due to changes in the radioactivity level over time. Arterial blood was continuously sampled for 5 min after each injection of IMP. One-point arterial blood sampling was also performed immediately before the second injection. Planar images were acquired at 5, 7 and 25 min after each IMP injection and immediately before the second injection.

#### Calculation of the $K_1$ values in the first and second sessions

The  $K_1$  values in the first and second sessions were calculated by a reference sample method based on a microsphere model.<sup>2</sup> SPECT data acquired 5 min after each injection of IMP were used with an input function calculated by integrating an arterial input curve over 5 min. To simulate the ME method described above, SPECT data acquired from 7 to 25 min after IMP injection were corrected to represent those at 5 min by using the radioactivity levels in the planar images at 5, 7 and 25 min. Thus, the  $K_1$  value in the first session was calculated from

$$K_1^I = \frac{A^I(5) \times \frac{C_b^I}{\alpha^I}}{\int_0^5 C_a(u) du}, \quad (7)$$

where

$$\alpha^I = \frac{A^I(7) + A^I(25)}{2}.$$

$C_b^I$  in Eq. (7) represents the level of brain radioactivity acquired by SPECT from 7 to 25 min, and was assumed to be calculated from

$$C_b^I = \frac{\int_7^{25} A^I(u) du}{25 - 7}.$$

Equation (7) is derived from Eq. (A2) in the Appendix, and  $A^I(5)$ ,  $A^I(7)$  and  $A^I(25)$  represent levels of brain radioactivity at 5, 7 and 25 min, respectively. These

values were actually obtained from the planar images and are shown as C5, C7 and C25, respectively, in Figure 1. The integration of  $C_a(t)$  over 5 min in Eq. (7) was actually obtained by 5-min continuous arterial blood sampling.

When estimating the  $K_1$  value in the second session, it is necessary to eliminate radioactivity remaining in the brain from the first session.<sup>5</sup> In this study, we considered the following four methods for estimating the  $K_1$  value in the second session (Fig. 2).

#### Method 1 [Fig. 2(a)]

With Method 1, the amount of radioactivity remaining in the brain from the first session [ $A^I(t_z)$ ] was simply subtracted from the level of brain radioactivity in the second session. An input function was generated by subtracting the arterial blood radioactivity level at the end of the first session [ $C_a^I(t_z)$ ] multiplied by 5 min, from the integrated arterial blood radioactivity level over a 5 min period after the second injection. This value is shown as a hatched area in Figure 2 (a). As in Eq. (7), SPECT data acquired from 7 to 25 min after the second injection of IMP were corrected to represent those at  $(t_z + 5)$  min by using the radioactivity levels at  $(t_z + 7)$  min and  $(t_z + 25)$  min. Thus, the  $K_1$  value in the second session was calculated from

$$K_1^{II} = \frac{A^{II}(t_z + 5) \times \frac{C_b^{II}}{\alpha^{II}} - A^I(t_z) \times \frac{C_b^I}{\alpha^I}}{\int_{t_z}^{t_z+5} C_a(u) du - C_a^I(t_z) \times 5}, \quad (8)$$

where

$$\alpha^{II} = \frac{A^{II}(t_z + 7) + A^{II}(t_z + 25)}{2}.$$

As in Eq. (7),  $C_b^{II}$  in Eq. (8) represents the brain radioactivity level acquired by SPECT from  $(t_z + 7)$  to  $(t_z + 25)$  min, and was assumed to be calculated from

$$C_b^{II} = \frac{\int_{t_z+7}^{t_z+25} A^{II}(u) du}{(t_z + 25) - (t_z + 7)}.$$

Equation (8) is derived from Eq. (A11) in the Appendix, and this method requires 5-min continuous arterial blood sampling twice and one-point arterial sampling once to obtain the  $K_1$  values in the first and second sessions.

#### Method 2 [Fig. 2(b)]

The radioactivity remaining in the brain from the first session was corrected in the manner described for Method 1, whereas an input function was generated by multiplying the integrated arterial blood radioactivity level over a 5 min period after the first injection by  $R$ , so that the  $K_1$  value in the second session was calculated by

$$K_1^{II} = \frac{A^{II}(t_z + 5) \times \frac{C_b^{II}}{\alpha^{II}} - A^I(t_z) \times \frac{C_b^I}{\alpha^I}}{R \times \int_0^5 C_a^I(u) du}. \quad (9)$$

Equation (9) is derived from Eq. (A12) in the Appendix. Since this method requires 5-min continuous arterial blood sampling only once, it appears to be less invasive than Method 1.

### Method 3 [Fig. 2(c)]

The amount of radioactivity remaining in the brain from the first session [ $A^I(t_z)$ ] was subtracted from the level of brain radioactivity in the second session after taking into account the decay of  $A^I(t_z)$  due to washout from the brain over 5 min during the second session. The decay of  $A^I(t_z)$  under the circumstance can be taken into account by multiplying by  $e^{-k_2'' \times 5}$ . This corresponds to the term  $A^I(t_z) \cdot e^{-k_2''(t-t_z)}$  in Eq. (A5) in the Appendix. However, since the  $k_2$  value in the second session is not known, the decay was estimated by using the  $K_1$  value estimated in the first session and the population averaged partition coefficient ( $= K_1/k_2$ ), so that the  $K_1$  value in the second session was calculated by

$$K_1'' = \frac{A''(t_z + 5) \times \frac{C_b''}{\alpha''} - A^I(t_z) \times \frac{C_b^I}{\alpha^I} \times e^{-K_1^I \times 5/\lambda}}{\int_{t_z}^{t_z+5} C_a(u) du} \quad (10)$$

$\lambda$  in Eq. 10 represents the population averaged partition coefficient. In this study, this value was fixed to 30.0 ml/g (the mean value obtained from our dynamic studies) or 39.1 ml/g (the mean value reported by Nishizawa et al.<sup>15</sup>). Equation (10) is derived from Eq. (A5) in the Appendix. In this method, the integrated arterial blood radioactivity over a period of 5 min after the second injection was taken as an input function, which is shown as hatching in Figure 2 (c). When using this method, 5-min continuous arterial blood sampling must be performed twice to obtain the  $K_1$  values in the first and second sessions.

### Method 4 [Fig. 2(d)]

With this method, the  $K_1$  value in the second session was calculated by

$$K_1'' = \frac{A''(t_z + 5) \times \frac{C_b''}{\alpha''} - A^I(t_z) \times \frac{C_b^I}{\alpha^I} \times e^{-\tilde{K}_1'' \times 5/\lambda}}{\int_{t_z}^{t_z+5} C_a(u) du} \quad (11)$$

This method is the same as Method 3 except that  $K_1^I$  in Eq. (10) was replaced by  $\tilde{K}_1''$  which represents the  $K_1$  value in the second session obtained by Method 2. Like Method 3, this procedure also requires two 5-min sessions of continuous arterial blood sampling.

### Simulation study based on patient data

#### SPECT procedure

We obtained patient data for simulation studies by using dynamic SPECT as follows. Dynamic SPECT studies were performed with a SPECT 2000H-40 (Hitachi Medical Co., Tokyo, Japan), which is a four-sided gamma camera arrangement equipped with a low-energy general-purpose collimator.<sup>16</sup> The head of the patient was posi-

tioned in the SPECT 2000H-40 scanner. Approximately 222 MBq of IMP was injected into an antecubital vein. The scanner was simultaneously started and arterial blood sampling was begun from a small catheter placed in the brachial artery. These arterial whole-blood samples were analyzed for the true tracer radioactivity [ $C_a(t)$ ] by octanol extraction.<sup>2,12</sup> Scanning progressed for about one hour (20 scans) with the duration of each scan being 160 sec. The transverse images were reconstructed by a filtered backprojection method with a Shepp-Logan filter. Attenuation was corrected by Chang's method. The SPECT counts and arterial blood radioactivity were corrected for decay and were mutually calibrated with a well-type scintillation counter.<sup>12</sup>

A total of 128 regions of interest (ROIs) were selected in bilateral frontal, temporal, temporo-occipital and occipital cortices on a slice through the basal ganglia in 16 patients with various brain diseases. The patients were 10 males and 6 females ranging in age from 22 to 70 years ( $56 \pm 11$  years). Informed consent was obtained from each of the patients before participation in the study.

### Simulation

We obtained the  $K_1$  and  $k_2$  values by fitting the time course of the level of IMP brain radioactivity measured by dynamic SPECT to Eq. (3), by the nonlinear least-squares method.<sup>17</sup> We simulated time-activity curves in the brain of the first and second sessions with the  $K_1$  and  $k_2$  values thus obtained with Eqs. (3) and (4), respectively. We simulated conditions when  $K_1$  and  $k_2$  did not change at all, and when they changed by 12% and 60% in the second session. Under these conditions, we assumed that the partition coefficient did not change during the second session.

The error between the estimated and assumed values for  $K_1$  in the second session was calculated with the following equation:

$$\text{Error} = \frac{K_1''(\text{estimated}) - K_1''(\text{assumed})}{K_1''(\text{assumed})} \times 100 (\%), \quad (12)$$

where  $K_1''(\text{assumed})$  and  $K_1''(\text{estimated})$  are the assumed and estimated  $K_1$  values in the second session, respectively. The percent change in  $K_1$  between the first and second sessions was defined as

$$\begin{aligned} &\text{Percent change} \\ &= \frac{K_1^I(\text{estimated}) - K_1^I(\text{assumed})}{K_1^I(\text{assumed})} \times 100 (\%), \quad (13) \end{aligned}$$

where  $K_1^I(\text{estimated})$  is the estimated  $K_1$  value in the first session.

### Clinical evaluation

Clinical evaluation was performed as follows. First, the reproducibility of two sequential measurements of  $K_1$  was

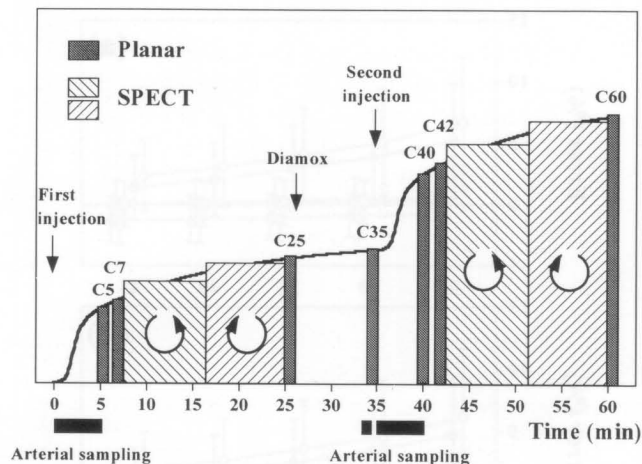


**Fig. 1** Protocol of the modified early (ME) method originally developed by Inoue et al.<sup>10</sup> when applied to split dose IMP SPECT. The second session starts 35 min after the first injection of IMP. SPECT data are acquired from 7 to 25 min after each injection of IMP by rotating a gamma camera twice clockwise and counterclockwise. Planar images are also acquired at 5, 7 and 25 min after each injection of IMP, and immediately before the second injection. Arterial blood is also sampled for a period of 5 min after each injection of IMP, and one-point arterial blood sampling proceeds immediately before the second injection.

assessed with clinical data obtained from six patients with cerebrovascular diseases (4 males, 2 females; age,  $63 \pm 13$  years) without any intervention (Fig. 7). This study was performed after obtaining informed consent from each of the patients.

Clinical data were acquired by the ME method as previously described (Fig. 1). With the ME method (Fig. 1),<sup>10</sup> dynamic frontal brain images were first acquired with the gamma camera (STARCAM 4000 XR/T, GE-Yokogawa Medical Systems, Tokyo, Japan) equipped with a low-energy general-purpose collimator after a bolus injection of IMP. The imaging protocol consisted of 28 frames in a  $64 \times 64$  matrix, each 15 sec in duration, for a total acquisition time of 7 min. At the same time, continuous arterial blood sampling from an indwelling catheter needle inserted in the brachial artery was performed for 5 min at a speed of 1.88 ml/min by means of a universal infusion system (Truth A-II, Nakagawa Seikoudo Co., Tokyo, Japan). After that, the SPECT data were acquired. Each projection image was acquired in 12 sec with a  $64 \times 64$  matrix as a 2.67-fold magnification and repeated 32 times during a 360-degree rotation.<sup>10</sup> This rotation was repeated twice, clockwise and counterclockwise. Reconstruction of images was performed by the filtered backprojection method with a ramp backprojection filter and a Butterworth filter (order = 8, cut-off frequency = 0.39 cycles/cm). Attenuation correction was performed

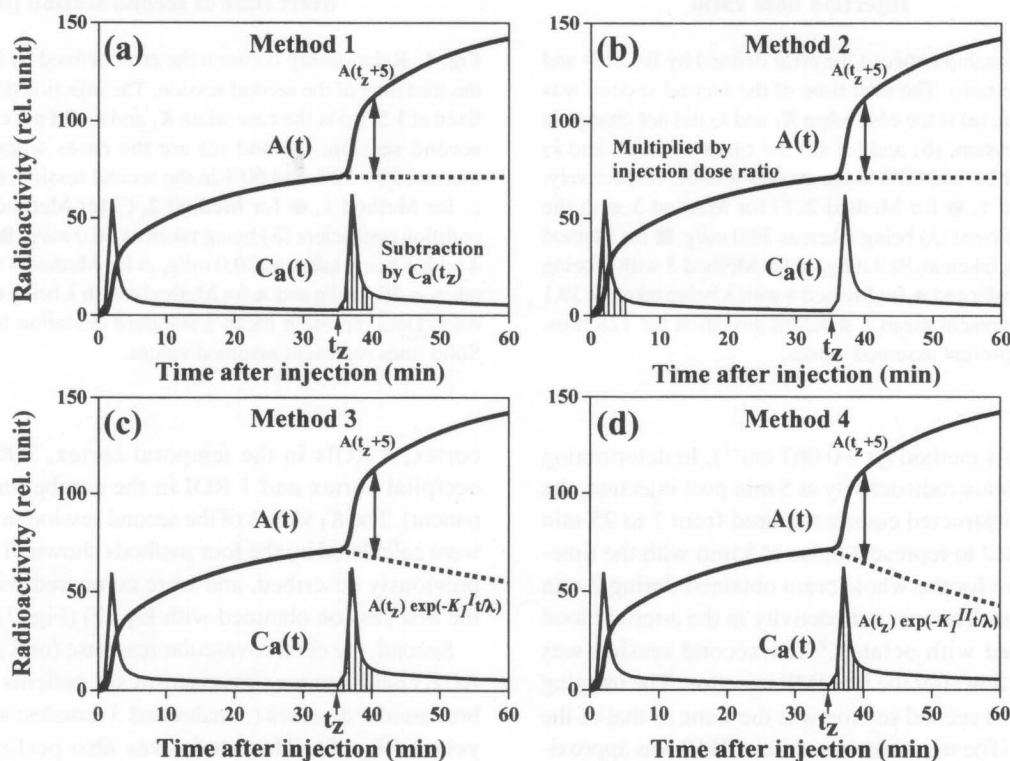


**Fig. 2** Four methods based on a microsphere model for sequentially measuring CBF with a double injection of IMP. These four methods differ with respect to eliminating radioactivity remaining in the brain from the first session. Hatched area represents an input function used for estimating the  $K_1$  value in the second session; (a) for Method 1, (b) for Method 2, (c) for Method 3 and (d) for Method 4.

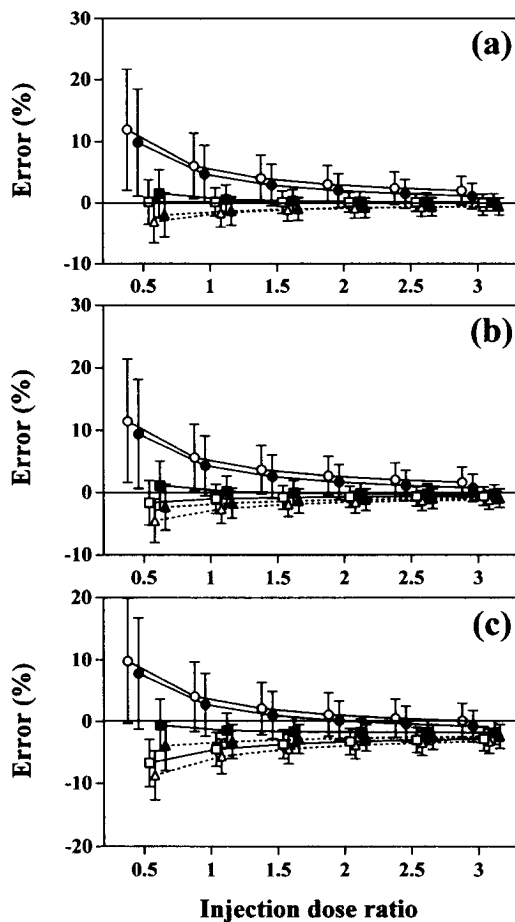


**Fig. 3** Relationship between the error defined by Eq. (12) and injection dose ratio. The start time of the second session was fixed at 35 min. (a) is the case when  $K_1$  and  $k_2$  did not change in the second session. (b) and (c) are the cases when  $K_1$  and  $k_2$  increased by 12% and 60% in the second session, respectively. ○ for Method 1, ● for Method 2, □ for Method 3 with the partition coefficient ( $\lambda$ ) being taken as 30.0 ml/g, ■ for Method 4 with  $\lambda$  being taken as 30.0 ml/g, △ for Method 3 with  $\lambda$  being taken as 39.1 ml/g and ▲ for Method 4 with  $\lambda$  being taken as 39.1 ml/g. Data represent mean  $\pm$  standard deviation for 128 runs. Solid lines represent assumed values.

by Sorenson's method ( $\mu = 0.067 \text{ cm}^{-1}$ ). In determining the level of brain radioactivity at 5 min post injection, the SPECT reconstructed counts acquired from 7 to 25 min were corrected to represent those at 5 min with the time-activity curve for the whole brain obtained during 7 min after injection. The true radioactivity in the arterial blood was extracted with octanol.<sup>2</sup> The second session was started at 35 min after the first IMP injection. The imaging protocol of the second session was the same as that of the first session. The total injection dose of IMP was approximately 222 MBq, and the injection dose ratio for the first and second sessions ranged from 1.41 to 1.56 ( $1.50 \pm 0.06$ ).

A total of 66 ROIs were selected (3 ROIs in the frontal

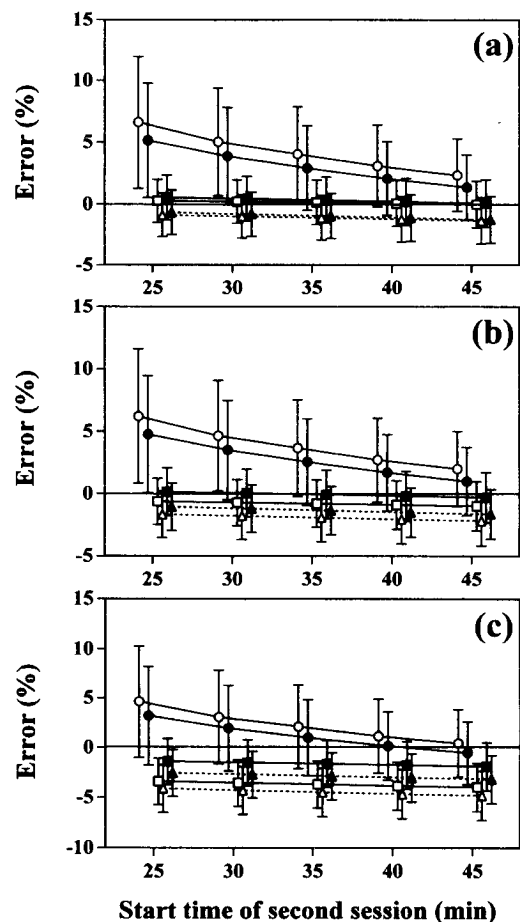


**Fig. 4** Relationship between the error defined by Eq. (12) and the start time of the second session. The injection dose ratio was fixed at 1.5. (a) is the case when  $K_1$  and  $k_2$  did not change in the second session. (b) and (c) are the cases when  $K_1$  and  $k_2$  increased by 12% and 60% in the second session, respectively. ○ for Method 1, ● for Method 2, □ for Method 3 with the partition coefficient ( $\lambda$ ) being taken as 30.0 ml/g, ■ for Method 4 with  $\lambda$  being taken as 30.0 ml/g, △ for Method 3 with  $\lambda$  being taken as 39.1 ml/g and ▲ for Method 4 with  $\lambda$  being taken as 39.1 ml/g. Data represent mean  $\pm$  standard deviation for 128 runs. Solid lines represent assumed values.

cortex, 4 ROIs in the temporal cortex, 3 ROIs in the occipital cortex and 1 ROI in the cerebellum for each patient). The  $K_1$  values of the second session in these ROIs were calculated by the four methods shown in Figure 2 as previously described, and were compared with those of the first session obtained with Eq. (7) (Fig. 7).

Second, the cerebrovascular response (or  $K_1$  change) to ACZ challenge was assessed in six patients with cerebrovascular diseases (3 males and 3 females; age,  $58 \pm 10$  years) (Fig. 8). This study was also performed after obtaining informed consent from each of the patients. At 26 min after the first IMP injection, one gram of ACZ (Diamox) was slowly administered intravenously (Fig. 1). The  $K_1$  values for the first and second sessions in the

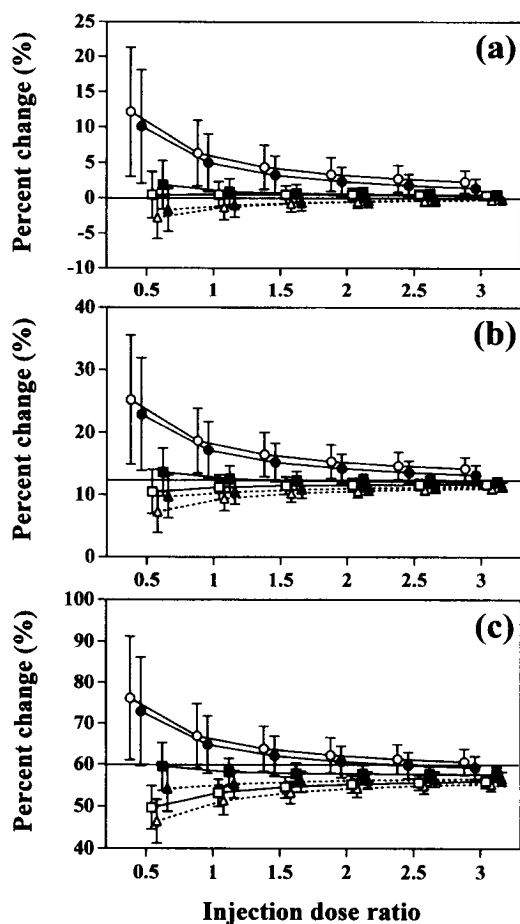


**Fig. 5** Relationship between the percent change defined by Eq. (13) and injection dose ratio. The start time of the second session was fixed at 35 min. (a) is the case when  $K_1$  and  $k_2$  did not change in the second session. (b) and (c) are the cases when  $K_1$  and  $k_2$  increased by 12% and 60% in the second session, respectively. ○ for Method 1, ● for Method 2, □ for Method 3 with the partition coefficient ( $\lambda$ ) being taken as 30.0 ml/g, ■ for Method 4 with  $\lambda$  being taken as 30.0 ml/g, △ for Method 3 with  $\lambda$  being taken as 39.1 ml/g and ▲ for Method 4 with  $\lambda$  being taken as 39.1 ml/g. Data represent mean  $\pm$  standard deviation for 128 runs. Solid lines represent assumed values.

nonischemic (24 ROIs) and ischemic regions (10 ROIs) were calculated with Eq. (7) and the four methods (Fig. 2), and the percent changes in  $K_1$  between the first and second sessions were calculated with Eq. (13) (Fig. 8).

#### Statistical analysis

The mean and standard deviation of the error and percent change defined by Eqs. (12) and (13), respectively, were calculated from 128 runs (Figs. 3–6). The correlations of the  $K_1$  values for the first and second sessions obtained without ACZ challenge were analyzed by linear regression analysis (Fig. 7). Statistical differences in the percent change in  $K_1$  between the first and second sessions after ACZ challenge were analyzed by Mann-Whitney's U test (Fig. 8). A p-value less than 0.05 was considered significant.

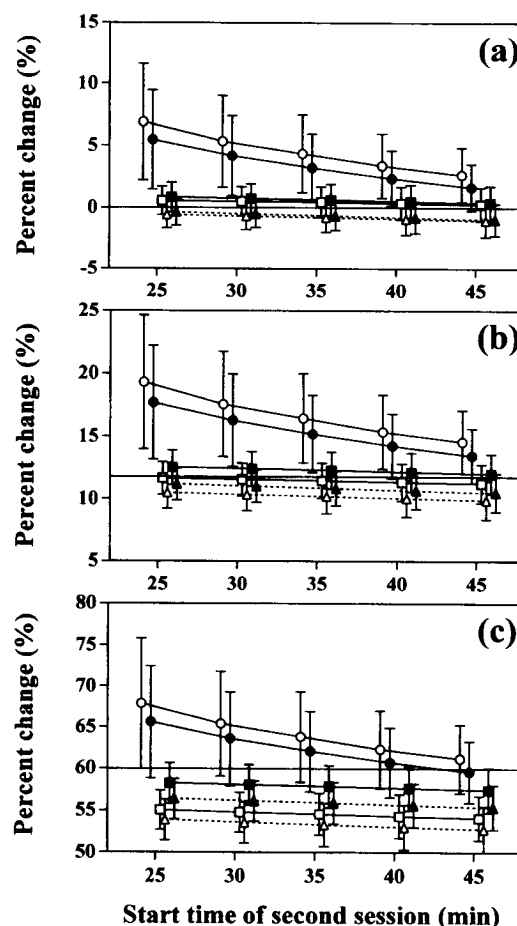


**Fig. 6** Relationship between the percent change defined by Eq. (13) and the start time of the second session. The injection dose ratio was fixed at 1.5. (a) is the case when  $K_1$  and  $k_2$  did not change in the second session. (b) and (c) are the cases when  $K_1$  and  $k_2$  increased by 12% and 60% in the second session, respectively. ○ for Method 1, ● for Method 2, □ for Method 3 with the partition coefficient ( $\lambda$ ) being taken as 30.0 ml/g, ■ for Method 4 with  $\lambda$  being taken as 30.0 ml/g, △ for Method 3 with  $\lambda$  being taken as 39.1 ml/g and ▲ for Method 4 with  $\lambda$  being taken as 39.1 ml/g. Data represent mean  $\pm$  standard deviation for 128 runs. Solid lines represent assumed values.

## RESULTS

#### Simulation study based on patient data

The kinetic parameters of IMP in 16 patients obtained by dynamic SPECT studies were as follows. The  $K_1$  values ranged from 0.1079 to 0.6583 ml/g/min, and the mean  $\pm$  SD was  $0.3320 \pm 0.0987$  ml/g/min. The  $k_2$  values ranged from 0.0047 to 0.0193 min<sup>-1</sup>, and the mean  $\pm$  SD was  $0.0113 \pm 0.0032$  min<sup>-1</sup>. The partition coefficient ( $= K_1/k_2$ ) ranged from 16.35 to 50.44 ml/g, and the mean  $\pm$  SD was  $30.00 \pm 6.84$  ml/g. These data were used in the following simulation studies.

The  $K_1$  values in the first session obtained from Eq. (7) and the assumed values closely correlated ( $r = 0.999$ ), but were underestimated by  $0.31 \pm 1.05\%$  compared with the

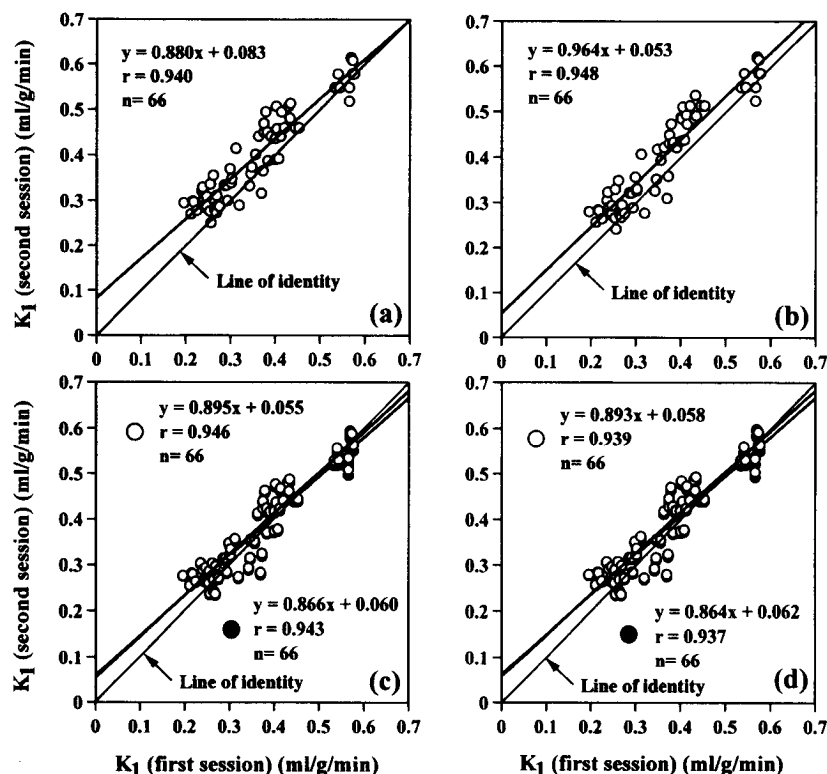


Fig. 7 Relationship between the  $K_1$  values in the first and second sessions obtained from six patients with cerebrovascular diseases by the four methods (Fig. 2) without any intervention. (a) for Method 1, (b) for Method 2, (c) for Method 3 and (d) for Method 4. ○ and ● in Figs. 7(c) and 7(d) represent the cases when  $\lambda$  was taken as 30.0 ml/g and 39.1 ml/g, respectively.

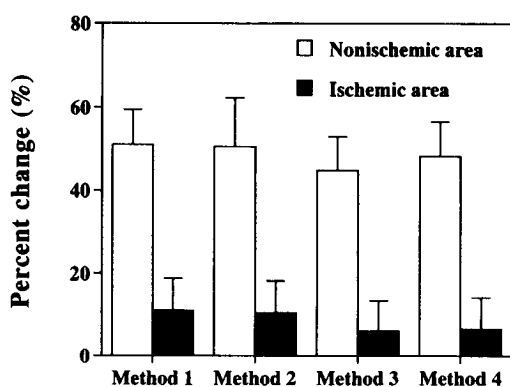


Fig. 8 Responses of  $K_1$  to acetazolamide challenge assessed by the four methods shown in Fig. 2. These data were obtained from six patients with cerebrovascular diseases and the percent change was calculated using Eq. (13). Data represent mean  $\pm$  standard deviation. □ for nonischemic area and ■ for ischemic area. Note that when using Methods 3 or 4,  $\lambda$  was taken as 30.0 ml/g. There was a significant difference between the nonischemic and ischemic areas for all methods. For the nonischemic area, the percent change obtained by Method 1 was significantly greater than that obtained by Method 3. For the ischemic area, there was no significant difference among the methods.

assumed values.

Figure 3 shows the relationship between the error in  $K_1$  in the second session calculated from Eq. (12) and  $R$ , whereas Figure 4 shows the relationship between the error and  $t_z$ . In these figures, (a) occurred when  $K_1$  and  $k_2$  did not change in the second session. When these parameters changed by 12% and 60% in the second session, (b) and (c) respectively resulted. The error in  $K_1$  estimated by Method 1 or 2 decreased with increasing  $R$  and  $t_z$ , whereas the accuracy of Method 3 or 4 did not largely depend on  $R$  and  $t_z$ . Furthermore, the standard deviation of the error in  $K_1$  estimated by Method 1 or 2 was always greater than that for Method 3 or 4. The  $K_1$  values in the second session obtained by Method 3 or 4 with  $\lambda$  being taken as 39.1 ml/g were always smaller by approximately 1–3% compared with those obtained by these methods with a  $\lambda$  value of 30.0 ml/g. The difference between the  $K_1$  values for the two situations decreased with increasing  $R$ , and did not depend on  $t_z$ . It should be noted that 30.0 ml/g is the mean value for  $\lambda$  obtained from our dynamic studies as previously described, and 39.1 ml/g is that reported by Nishizawa et al.<sup>15</sup>

Figure 5 shows the percent change calculated from Eq. (13) as a function of  $R$ , whereas Fig. 6 shows that as a function of  $t_z$ . As in Figs. 3 and 4, (a) resulted when  $K_1$  and  $k_2$  did not change in the second session. When these



parameters increased by 12% and 60% in the second session, (b) and (c), respectively, resulted. The standard deviation of the percent change estimated by Method 1 or 2 was greater than that estimated by Method 3 or 4. Furthermore, the percent change estimated by Method 1 or 2 largely depended on  $R$  and approached the assumed value with increasing  $R$ . The percent change estimated by Method 3 or 4 also depended on  $R$ , but to a much lesser extent than that by Method 1 or 2. The percent change estimated by Method 1 or 2 decreased with increasing  $t_z$ , whereas that for Method 3 or 4 remained almost constant regardless of the  $t_z$  value.

#### Clinical evaluation

Figure 7 shows the relationship between the  $K_1$  values in the first and second sessions obtained by the four methods without any intervention [(a) for Method 1, (b) for Method 2, (c) for Method 3 and (d) for Method 4].  $\circ$  and  $\bullet$  in Figures 7(c) and 7(d) represent the cases when  $\lambda$  was taken as 30.0 ml/g and 39.1 ml/g, respectively. There was a significant correlation between them for all methods (Fig. 7). With Method 1 or 2 [Figs. 7(a) and 7(b)], there was a tendency for the  $K_1$  values in the second session to be overestimated compared with those in the first session. As shown by  $\circ$  and  $\bullet$  in Figures 7(c) and 7(d), the relationship between the  $K_1$  values in the first and second sessions obtained by Method 3 or 4 did not largely depend on  $\lambda$ .

Figure 8 shows the responses of  $K_1$  to ACZ challenge assessed by the four methods ( $\square$  for a nonischemic area and  $\blacksquare$  for an ischemic area). When using Method 3 or 4,  $\lambda$  was taken as 30.0 ml/g. There was a significant difference in the response between the nonischemic and ischemic areas for all methods. For the nonischemic area, the percent change in the  $K_1$  value obtained by Method 1 was significantly greater than that obtained by Method 3. For the ischemic area, there was no significant difference among the methods. When using Method 3 or 4, there was no significant difference between the results obtained by taking  $\lambda$  as 30.0 ml/g and 39.1 ml/g (data not shown).

## DISCUSSION

Various methods for quantifying CBF with IMP have been proposed.<sup>2,18–22</sup> The most popular method is that based on a microsphere model.<sup>2</sup> Ohkubo et al.<sup>23</sup> demonstrated that a method based on the microsphere model is the most accurate and reliable among the various proposed methods, but when applying the microsphere method to split dose IMP SPECT, the second measurement must be particularly affected by the inherent characteristics of IMP, namely its gradual washout from the brain.<sup>15</sup> It therefore appears important to understand the extent of this effect on the accuracy of CBF measurement with a double injection of IMP.

The kinetic behavior of IMP in the human brain can be described by a two-compartment model.<sup>12</sup> Our recent

studies with spectral analysis also supported the above notion.<sup>24</sup> We therefore calculated the level of IMP radioactivity in the brain based on a two-compartment model [Eqs. (3) and (4)]. In the present simulation studies, we assumed that the partition coefficient did not change during the second session even when simulating activation studies. This assumption is derived from the fact that the partition coefficient is almost the same during activation with ACZ as shown by Nishizawa et al.<sup>15</sup> Furthermore, when calculating the level of brain radioactivity in the second session [Eq. (4)], we also assumed that the rate constant instantaneously changes between the first and second sessions. In fact, the rate constants are likely to adjust gradually,<sup>25</sup> although the actual rate of change is not known, but we believe that this assumption is permissible for the purpose of this study.

We also assumed that the level of radioactivity in arterial blood due to the second injection [ $C_a^{II}(t)$ ] is given by Eq. (6). Although this assumption may not always hold true in clinical settings, we believe that it is valid for the purpose of our simulation study. Inoue et al.<sup>10</sup> investigated the correlation between the measured arterial blood radioactivity due to the second injection and that calculated from the first arterial blood radioactivity multiplied by the injection dose ratio, and reported that there was an excellent correlation between them ( $r = 0.981$ ,  $n = 7$ ). This suggests that the above assumption is also applicable in clinical settings.

Hashikawa et al.<sup>5</sup> used a procedure similar to Method 1 for calculating the mean CBF values in the second session, and found good reproducibility between the first and second CBF values in rest-rest studies ( $r = 0.915$ ,  $n = 20$ ). On the other hand, Inoue et al.<sup>10</sup> used Method 2, and they also reported good reproducibility in rest-rest studies ( $r = 0.924$ ,  $n = 16$ ), but our results (Figs. 3 and 4) indicated that the accuracy of Method 1 or 2 largely depends on  $R$  and  $t_z$ . In addition, our results (Figs. 5 and 6) indicated that the change in  $K_1$  during the second session estimated by these methods also largely depends on  $R$  and  $t_z$ . This means that when  $R$  and  $t_z$  are considered to be smaller, these methods are more affected by the radioactivity remaining from the first session. Our results therefore suggest that  $R$  and  $t_z$  should be carefully considered when using these methods. To reduce the effect of the radioactivity remaining from the first session,  $t_z$  should be taken as large as possible. This, however, will result in increasing the total examination time and the burden on the patient.  $t_z$  should therefore be determined from a compromise between the accuracy of the data and the burden on the patient.  $R$  should also be as large as possible for this purpose, but when  $R$  is taken as being larger, the signal-to-noise (S/N) ratio in the CBF image of the first session appears to deteriorate more. We therefore investigated the relationship between  $R$  and the S/N ratio in CBF images by phantom experiments. Although the data are not shown here, the S/N ratios in the images from the first and second

sessions decreased and increased, respectively, with increasing  $R$ . If the optimal injection dose ratio is assumed to be the ratio at which the S/N ratio in the first session is equal to that in the second, then the injection dose ratio was approximately 1.5 to 2.0. Our previous investigations showed that the optimal injection dose ratio is approximately 1.8 when mapping changes in cerebral glucose utilization by means of fluorine-18 fluorodeoxyglucose double injection and the constrained weighted-integration method.<sup>26</sup> This value is very similar to that obtained here.

With Method 3 or 4, the effect of the IMP washout from the brain in the second session was corrected by using the population averaged partition coefficient [Eqs. (10) and (11)]. With Method 3, the  $K_1$  value in the first session was used for the above correction [Eq. (10)], and with Method 4, the  $K_1$  value in the second session obtained by Method 2 was used for the correction [Eq. (11)], suggesting that Method 4 is theoretically better than Method 3. Although Method 4 is more complex than Method 3, Method 4 seems to be more accurate, especially when the change in  $K_1$  during the second session is large (Figs. 4 and 6). As previously mentioned, the partition coefficient obtained from dynamic SPECT studies of 16 patients was  $30.00 \pm 6.84$  ml/g. On the other hand, Nishizawa et al.<sup>15</sup> reported a mean value of 39.1 ml/g, which was obtained from 15 patients. Ohkubo et al.<sup>23</sup> have reported  $28.0 \pm 7.0$  ml/g which was obtained from 15 individuals by means of the nonlinear least squares fitting analysis. Our mean value for the partition coefficient was smaller than that of Nishizawa et al.,<sup>15</sup> but it was very similar to that of Ohkubo et al.<sup>23</sup> We therefore investigated two conditions in which the partition coefficient was fixed at 30 ml/g or 39.1 ml/g in Method 3 or 4. As previously described, the  $K_1$  values in the second session obtained by taking  $\lambda$  as 39.1 ml/g were about 1–3% smaller than those obtained when  $\lambda$  was taken as 30 ml/g. As shown in Figures 3 and 5, the difference between the two situations decreased with increasing  $R$ , suggesting that taking a large  $R$  value is also effective for these methods. Even if the partition coefficient is fixed to the population averaged value, the standard deviation of the error and percent change in the  $K_1$  values estimated by Method 3 or 4 is smaller than that for Method 1 or 2 (Figs. 3–6), suggesting that these methods are more reliable than Method 1 or 2.

The accuracy of Method 3 or 4 somewhat depended on  $R$  when  $R$  was less than 1.0 (Figs. 3 and 5), but to a much lesser extent than that for Method 1 or 2. In addition, there was no great dependence on  $t_z$  in Method 3 or 4 (Figs. 4 and 6). This aspect will be helpful for reducing the total examination time, thus lessening the burden on the patient.

Although Method 3 or 4 appears to be more reliable than Method 1 or 2, they require 5-min continuous arterial blood sampling twice. On the other hand, with Method 2, the 5-min continuous arterial blood sampling in the sec-

ond session can be omitted by using the injection dose ratio. Method 2 therefore appears to be somewhat superior to other methods in terms of noninvasiveness and simplicity. We have recently developed a method in which 5-min continuous arterial blood sampling can be replaced by a one-point sampling.<sup>27</sup> If this approach were applied, Method 2 would become even less invasive. Although Method 2 has the drawback that its accuracy largely depends on  $R$  and  $t_z$ , this procedure also appears attractive for routine clinical use.

In our clinical settings,  $t_z$  is fixed at 35 min in order to make the total examination time as short as possible. From the simulation results shown in Figure 4, Method 1 or 2 is expected to somewhat overestimate the  $K_1$  value in the second session when  $t_z$  is taken as 35 min. Actually, the  $K_1$  values in the second session obtained by Method 1 or 2 were overestimated compared with those in the first session [Figs. 7(a) and 7(b)]. In Method 1 or 2, the radioactivity remaining in the arterial blood from the first session is eliminated when calculating the  $K_1$  value in the second session, as previously mentioned, so that the input function [denominator in Eqs. (8) or (9)] appears to be underestimated when  $t_z$  is 35 min. This is probably the main reason why the  $K_1$  values in the second session obtained by these methods were overestimated compared with those in the first session. To reduce this overestimation,  $t_z$  should have been taken as larger, as suggested by the simulation studies (Fig. 4). On the other hand, although some scatter of the data is observed, the reproducibility of two sequential measurements of  $K_1$  using Method 3 or 4 appears good and does not largely depend on  $\lambda$  [Figs. 7(c) and 7(d)], suggesting that Method 3 or 4 is more reliable than Method 1 or 2. If the variation in  $\lambda$  is within the range of that in the reported  $\lambda$  values,<sup>15,23</sup> this effect on the accuracy of Method 3 or 4 appears to be small. The above results are consistent with those obtained by simulation studies, but Figure 8 shows that any method can provide reasonable estimation of response to ACZ and significant difference in the response between the nonischemic and ischemic areas, which are comparable to those obtained by <sup>133</sup>Xe-SPECT.<sup>6</sup> These results suggest that although there are some drawbacks in Method 1 or 2 as previously mentioned, these methods can also be routinely used for assessment of perfusion reserve with ACZ challenge.

## CONCLUSION

We investigated the accuracy of a double-injection method for sequentially measuring CBF with IMP in simulation studies based on the patient data and in clinical studies. We considered four methods based on a microsphere model, and focused on the effects of  $R$  and  $t_z$  on their accuracy. Theoretically, Method 4 appears to be the best of the four methods. Our simulation results suggest that Method 3 or 4 can estimate changes in CBF during the

second session more reliably than Method 1 or 2, without largely depending on  $R$  and  $t_z$ . On the other hand, when using Method 1 or 2,  $R$  and  $t_z$  should be carefully considered. Since Method 2 is somewhat superior to other procedures in terms of noninvasiveness and simplicity, it also has the potential for routine clinical use. We believe that the findings of this study will be helpful when selecting a method with which to sequentially measure CBF with a double injection of IMP.

## APPENDIX

When applying a microsphere model, that is, assuming that the IMP washout from the brain can be neglected, Eq. (3) is reduced to

$$A'(t) \approx K_1' \cdot \int_0^t C_a(u) du, \quad (A1)$$

yielding

$$K_1' \approx \frac{A'(t)}{\int_0^t C_a(u) du}. \quad (A2)$$

Equation (4) can be rearranged as

$$A''(t) = A'(t_z) \cdot e^{-k_2''(t-t_z)} + K_1'' \cdot \int_{t_z}^t e^{-k_2''(t-u)} C_a(u) du, \quad (A3)$$

where

$$A'(t_z) = K_1' \cdot \int_0^{t_z} e^{-k_2''(t_z-u)} C_a(u) du.$$

The first term on the right-hand side of Eq. (A3) represents the level of radioactivity remaining in the brain from the first session, with the decay due to washout from the brain being taken into account. When applying the same assumption as in Eq. (A1) to Eq. (A3), Eq. (A3) is reduced to

$$A''(t) \approx A'(t_z) \cdot e^{-k_2''(t-t_z)} + K_1'' \cdot \int_{t_z}^t C_a(u) du. \quad (A4)$$

It should be noted that the error in  $A''(t)$  caused by taking the  $k_2''$  value in the first term on the right-hand side of Eq. (A3) as zero, is larger by a factor of approximately 3 to 4 than that caused by taking the  $k_2''$  value in the second term as zero, so that the  $k_2''$  value in the first term on the right-hand side of Eq. (A3) cannot be neglected compared with that in the second term. From Eq. (A4),  $K_1''$  can be obtained by

$$K_1'' \approx \frac{A''(t) - A'(t_z) \cdot e^{-k_2''(t-t_z)}}{\int_{t_z}^t C_a(u) du}. \quad (A5)$$

Methods 3 and 4 are based on Eq. (A5). If the partition coefficient  $\lambda$  ( $= K_1''/k_2''$ ) is introduced, Eq. (A5) becomes

$$K_1'' \approx \frac{A''(t) - A'(t_z) \cdot e^{-K_1''(t-t_z)/\lambda}}{\int_{t_z}^t C_a(u) du}. \quad (A6)$$

In Method 3,  $K_1''$  on the right-hand side of Eq. (A6) is replaced by  $K_1'$ , whereas in Method 4 it is replaced by the  $K_1$  value in the second session obtained by Method 2.

Furthermore, Eq. (A4) can be rearranged as

$$A''(t) \approx A'(t_z) - A'(t_z) \cdot [1 - e^{-k_2''(t-t_z)}] + K_1'' \cdot \int_{t_z}^t C_a(u) du. \quad (A7)$$

The second term on the right-hand side of Eq. (A7) represents the change in the radioactivity level remaining in the brain from the first session due to washout. If we assume that this change is canceled out by the radioactivity uptaken by the brain from the radioactivity remaining in the arterial blood from the first session, that is,

$$A'(t_z) \cdot [1 - e^{-k_2''(t-t_z)}] \approx K_1'' \cdot \int_{t_z}^t C_a(u) du. \quad (A8)$$

Eq. (A7) is reduced to

$$A''(t) \approx A'(t_z) + K_1'' \cdot \left[ \int_{t_z}^t C_a(u) du - \int_{t_z}^t C_a(u) du \right]. \quad (A9)$$

When  $C_a'(t)$  is assumed to be nearly equal to  $C_a'(t_z)$  for  $t > t_z$ , Eq. (A9) is reduced to

$$A''(t) \approx A'(t_z) + K_1'' \cdot \left[ \int_{t_z}^t C_a(u) du - (t - t_z) \cdot C_a'(t_z) \right]. \quad (A10)$$

Thus, from Eq. (A10), we obtain

$$K_1'' \approx \frac{A''(t) - A'(t_z)}{\int_{t_z}^t C_a(u) du - (t - t_z) \cdot C_a'(t_z)}. \quad (A11)$$

Method 1 is based on Eq. (A11). When using Eqs. (5) and (6) for  $C_a(t)$  in Eq. (A11), we obtain

$$K_1'' \approx \frac{A''(t) - A'(t_z)}{R \cdot \int_0^{t-t_z} C_a'(u) du}. \quad (A12)$$

Method 2 is based on Eq. (A12).

## REFERENCES

- Winchell HS, Baldwin RM, Lin TH. Development of I-123-labeled amines for brain studies: localization of I-123 iodophenylalkyl amines in rat brain. *J Nucl Med* 21: 940-946, 1980.
- Kuhl DE, Barrio JR, Huang SC, Selin C, Ackermann RF, Lear JL, et al. Quantifying local cerebral blood flow by N-isopropyl-p-[<sup>123</sup>I]iodoamphetamine (IMP) tomography. *J Nucl Med* 23: 196-203, 1982.
- Vorstrup S. Tomographic cerebral blood flow measurements in patients with ischemic cerebrovascular disease and evaluation of the vasodilatory capacity by the acetazolamide test. *Acta Neurol Scand* 114: 1-47, 1988.
- Buell U, Schicha H. Nuclear medicine to image applied pathophysiology: evaluation of reserves by emission computerized tomography. *Eur J Nucl Med* 16: 129-135, 1990.
- Hashikawa K, Matsumoto M, Moriwaki H, Oku N, Okazaki Y, Uehara T, et al. Split dose iodine-123-IMP SPECT: sequential quantitative regional cerebral blood flow change with pharmacological intervention. *J Nucl Med* 35: 1226-1233, 1994.
- Chollet F, Celsis P, Clanet M, Guiraud-Chaumeil B, Rascal A, Marc-Vergnes JP. SPECT study of cerebral blood flow reactivity after ACZ in patients with transient ischemic attacks. *Stroke* 20: 458-464, 1989.
- Matsuda H, Higashi S, Kinuya K, Tsuji S, Nozaki J, Sumiya

- H, et al. SPECT evaluation of brain perfusion reserve by the ACZ test using  $^{99m}\text{Tc}$ -HMPAO. *Clin Nucl Med* 16: 572–579, 1991.
8. Hattori N, Yonekura Y, Tanaka F, Fujita T, Wang J, Ishizu K, et al. One-day protocol for cerebral perfusion reserve with acetazolamide. *J Nucl Med* 37: 2057–2061, 1996.
9. Moriwaki H, Matsumoto M, Hashikawa K, Oku N, Ishida M, Seike Y, et al. Hemodynamic aspect of cerebral watershed infarction: assessment of perfusion reserve using iodine-123-iodoamphetamine SPECT. *J Nucl Med* 38: 1556–1562, 1997.
10. Inoue T, Fujioka H, Akamune A, Tanada S, Hamamoto K. A time-saving approach for quantifying regional cerebral blood flow and application to split-dose method with  $^{123}\text{I}$ -IMP SPECT using a single-head rotating gamma-camera. *KAKU IGAKU (Jpn J Nucl Med)* 32: 1217–1226, 1995. (in Japanese)
11. Nishizawa S, Tanada S, Yonekura Y, Fujita T, Mukai T, Saji H, et al. Regional dynamics of N-isopropyl-( $^{123}\text{I}$ )p-iodoamphetamine in human brain. *J Nucl Med* 30: 150–156, 1989.
12. Murase K, Tanada S, Mogami H, Kawamura M, Miyagawa M, Yamada M, et al. Validity of microsphere model in cerebral blood flow measurement using N-isopropyl-p-(I-123)iodoamphetamine. *Med Phys* 17: 79–83, 1990.
13. Murase K, Tanada S, Inoue T, Ochi K, Fujita H, Sakaki S, et al. Measurement of the blood-brain barrier permeability of I-123 IMP, Tc-99m HMPAO and Tc-99m ECD in the human brain using compartment model analysis and dynamic SPECT. *J Nucl Med* 32: 911, 1991. (abstract)
14. Matsuda H, Seki H, Sumiya H, Tsuji S, Tonami N, Hisada K, et al. Quantitative cerebral blood flow measurements using N-isopropyl-(iodine 123)p-iodoamphetamine and single photon emission computed tomography with rotating gamma camera. *Am J Physiol Imaging* 1: 186–194, 1986.
15. Nishizawa S, Yonekura Y, Tanaka F, Fujita T, Tsuchimochi S, Ishizu K, et al. Evaluation of a double-injection method for sequential measurement of cerebral blood flow with iodine-123-iodoamphetamine. *J Nucl Med* 36: 1339–1345, 1995.
16. Kimura K, Hashikawa K, Etani H, Uehara A, Kozuka T, Moriwaki H, et al. A new apparatus for brain imaging: four-head rotating gamma camera single-photon emission computed tomograph. *J Nucl Med* 31: 603–609, 1990.
17. Beck JV, Arnold KJ. *Parameter Estimation in Engineering and Science*. New York: John Wiley & Sons, 1977.
18. Podreka I, Baumgartner C, Suess E, Muller C, Brucke T, Lang W, et al. Quantification of regional cerebral blood flow with IMP-SPECT: reproducibility and clinical relevance. *Stroke* 20: 183–191, 1989.
19. Yonekura Y, Iwasaki Y, Fujita T, Sasayama S, Matoba N, Sadato N, et al. Simple quantification of regional brain perfusion SPECT and IMP using a large field gamma camera. *KAKU IGAKU (Jpn J Nucl Med)* 27: 1311–1316, 1990. (in Japanese)
20. Takeshita G, Maeda H, Nakane K, Toyama H, Sakakibara E, Komai S, et al. Quantitative measurement of regional cerebral blood flow using N-isopropyl-(iodine-123)p-iodoamphetamine and single-photon emission computed tomography. *J Nucl Med* 33: 1741–1749, 1992.
21. Yokoi T, Iida H, Itoh H. A new graphic plot analysis for cerebral blood flow and partition coefficient with iodine-123-iodoamphetamine and dynamic SPECT: validation studies using oxygen-15-water and PET. *J Nucl Med* 34: 498–505, 1993.
22. Iida H, Itoh H, Nakazawa M. Quantitative mapping of regional cerebral blood flow using iodine-123-IMP and SPECT. *J Nucl Med* 35: 2019–2030, 1994.
23. Ohkubo M, Odano I, Takahashi M. A comparative study of simple methods to measure regional cerebral blood flow using iodine-123-IMP SPECT. *J Nucl Med* 38: 597–601, 1997.
24. Murase K, Tanada S, Inoue T, Ikezoe J. Spectral analysis applied to dynamic single photon emission computed tomography studies with N-isopropyl-p-( $^{123}\text{I}$ )iodoamphetamine. *Ann Nucl Med* 12: 109–114, 1998.
25. Dahl A, Russell D, Rootwelt K, Nyberg-Hansen R, Kerty E. Cerebral vasoreactivity assessed with transcranial Doppler and regional cerebral blood flow measurements. *Stroke* 26: 2302–2306, 1995.
26. Murase K, Kuwabara H, Yasuhara Y, Evans AC, Gjedde A. Mapping of change in cerebral glucose utilization using fluorine-18 fluorodeoxyglucose double injection and the constrained weighted-integration method. *IEEE Trans Med Imag* 15: 824–835, 1996.
27. Fujioka H, Murase K, Inoue T, Ishimaru Y, Akamune A, Yamamoto Y, et al. A method to estimate the integral of input function for the quantification of cerebral blood flow with  $^{123}\text{I}$ -IMP using one-point arterial blood sampling. *Nucl Med Commun* 19: 561–566, 1998.